J|A|C|S
ARTICLES
Published on Web 02/19/2002

Collagen Stability: Insights from NMR Spectroscopic and Hybrid Density Functional Computational Investigations of the Effect of Electronegative Substituents on Prolyl Ring Conformations

Michele L. DeRider,[†,‡] Steven J. Wilkens,[§] Michael J. Waddell,[⊥] Lynn E. Bretscher,[⊥,∥] Frank Weinhold,[†] Ronald T. Raines,*[,†,⊥] and John L. Markley*[,⊥]

Contribution from the Department of Chemistry, Graduate Program in Biophysics, and Department of Biochemistry, University of Wisconsin—Madison, Madison, Wisconsin 53706

Received July 23, 2001

Abstract: Collagen-like peptides of the type (Pro-Pro-Gly)$_{10}$ fold into stable triple helices. An electron-withdrawing substituent at the H$^{\gamma 3}$ ring position of the second proline residue stabilizes these triple helices. The aim of this study was to reveal the structural and energetic origins of this effect. The approach was to obtain experimental NMR data on model systems and to use these results to validate computational chemical analyses of these systems. The most striking effects of an electron-withdrawing substituent are on the ring pucker of the substituted proline (Pro$_i$) and on the trans/cis ratio of the Xaa$_{i-1}$—Pro$_i$ peptide bond. NMR experiments demonstrated that *N*-acetylproline methyl ester (AcProOMe) exists in both the C$^{\gamma}$-endo and C$^{\gamma}$-exo conformations (with the endo conformation slightly preferred), *N*-acetyl-4(*R*)-fluoroproline methyl ester (Ac-4*R*-FlpOMe) exists almost exclusively in the C$^{\gamma}$-exo conformation, and *N*-acetyl-4(*S*)-fluoroproline methyl ester (Ac-4*S*-FlpOMe) exists almost exclusively in the C$^{\gamma}$-endo conformation. In dioxane, the $K_{trans/cis}$ values for AcProOMe, Ac-4*R*-FlpOMe, and Ac-4*S*-FlpOMe are 3.0, 4.0, and 1.2, respectively. Density functional theory (DFT) calculations with the (hybrid) B3LYP method were in good agreement with the experimental data. Computational analysis with the natural bond orbital (NBO) paradigm shows that the pucker preference of the substituted prolyl ring is due to the gauche effect. The backbone torsional angles, ϕ and ψ, were shown to correlate with ring pucker, which in turn correlates with the known ϕ and ψ angles in collagen-like peptides. The difference in $K_{trans/cis}$ between AcProOMe and Ac-4*R*-FlpOMe is due to an n $\rightarrow \pi^*$ interaction associated with the Bürgi—Dunitz trajectory. The decrease in $K_{trans/cis}$ for Ac-4*S*-FlpOMe can be explained by destabilization of the trans isomer because of unfavorable electronic and steric interactions. Analysis of the results herein along with the structures of collagen-like peptides has led to a theory that links collagen stability to the interplay between the pyrrolidine ring pucker, ϕ and ψ torsional angles, and peptide bond trans/cis ratio of substituted proline residues.

Introduction

The conformational equilibria of flexible molecules arise from a complex balance of factors: primarily, steric hindrance, hyperconjugative delocalization, and long-distance nonbonded interactions (e.g., hydrogen bonding). In the amino acid proline, the balance among these factors can be altered drastically by the addition of an electronegative substituent to the prolyl ring. Proline is an abundant amino acid in collagen, which in turn is the most abundant protein in animals. Collagen consists of three polypeptide chains that form an extended right-handed triple helix. Each polypeptide chain is composed of approximately 300 repeats of the sequence Xaa-Yaa-Gly, where Xaa often is proline (Pro) and Yaa frequently is either Pro or 4(*R*)-hydroxyproline (4*R*-Hyp). Hydroxylation of Pro at the 4*R* position is known to lead to a substantial increase in the thermal stability of collagen.[1] Studies of collagen mimics, consisting of three strands of (Pro-Yaa-Gly)$_{10}$, have indicated that this increased stability arises, for the most part, from the inductive effects of an electronegative substituent in the 4*R* position, as in 4(*R*)-fluoroproline (4*R*-Flp).[2−4]

* To whom correspondence should be addressed. (R.T.R.) E-mail: raines@biochem.wisc.edu. Telephone: (608) 262-8588. Fax: (608) 262-3453. (J.L.M.) E-mail: markley@nmrfam.wisc.edu. Telephone: (608) 263-9349. Fax: (608) 262-3173.

† Department of Chemistry, University of Wisconsin—Madison.

‡ Current address: Department of Biochemistry, North Carolina State University, P.O. Box 7622, Raleigh, NC 27695.

§ Graduate Program in Biophysics, University of Wisconsin—Madison. Current address: Genomics Institute of the Novartis Research Foundation, 3115 Merryfield Row, Suite 200, San Diego, CA 92121.

⊥ Department of Biochemistry, University of Wisconsin—Madison.

∥ Current address: Department of Biochemistry, Medical College of Wisconsin, Milwaukee, WI 53226.

(1) Berg, R. A.; Prockop, D. J. *Biochem. Biophys. Res. Commun.* **1973**, *52*, 115−120.
(2) Holmgren, S. K.; Taylor, K. M.; Bretscher, L. E.; Raines, R. T. *Nature (London)* **1998**, *392*, 666−667.
(3) Holmgren, S. K.; Bretscher, L. E.; Taylor, K. M.; Raines, R. T. *Chem. Biol.* **1999**, *6*, 63−70.
(4) For a review on the conformational stability of the collagen triple helix, see: Jenkins, C. L.; Raines, R. T. *Nat. Prod. Rep.* **2002**, *19*, 49−59.

Table 1. Summary of Thermal Stability Data Collected from the Literature for Collagen Mimics Consisting of Three Chains of $(Xaa\text{-}Yaa\text{-}Gly)_n$

n	Xaa	Yaa	T_m (°C)	ref
7	Pro	Pro	6−7	10
10	Pro	Pro	41	2
7	Pro	4*R*-Hyp	36	9
10	Pro	4*R*-Hyp	69	2
7	Pro	4*R*-Flp	45	9
10	Pro	4*R*-Flp	91	2
7	Pro	4*S*-Flp	<2	9
10	4*R*-Hyp	Pro	<0	6

Both the position of the residue containing the electronegative substituent and the stereochemistry of that electronegative substituent play a role in triple-helix stability. The positional effects of γ-substitution are illustrated by the stabilities, relative to $(Pro\text{-}Pro\text{-}Gly)_{10}$, of $(Pro\text{-}4R\text{Hyp-}Gly)_{10}$ (increased triple-helix stability) and $(4R\text{Hyp-}Pro\text{-}Gly)_{10}$ (decreased stability).[5,6] The stereochemical effect of a γ-substituent is evident from a comparison of $(Pro\text{-}4R\text{Flp-}Gly)_7$, which forms a highly stable triple helix, and $(Pro\text{-}4S\text{Flp-}Gly)_7$, which fails to form a stable triple helix.[7−9] The data from these stability studies are compiled in Table 1.

Other factors that influence the stability of collagen are the trans/cis ratio of the $Xaa_{i-1}-Pro_i$ peptide bond and the ring pucker of Pro_i. The trans/cis ratio is important because all of the peptide bonds in triple-helical collagen reside in the trans conformation. In solution, proline can adopt one or both of the two possible ring puckers: endo (or "down") and exo (or "up") (Figures 1 and 2). In the Pro-Pro-Gly units of collagen mimics, the first proline prefers an endo ring pucker, and the second proline prefers an exo ring pucker.[11−18] This ring pucker preference could elicit changes in the main-chain torsion angles ϕ ($C'_{i-1}-N_i-C^{\alpha}{}_i-C'_i$) and ψ ($N_i-C^{\alpha}{}_i-C'_i-N_{i+1}$).[18]

Steric repulsion is perhaps the most intuitively understood factor in molecular conformational stability. Simply put, two atoms cannot occupy the same space. More precisely, like-spin electrons cannot occupy the same orbital (the Pauli exclusion principle). Such "Pauli repulsions" can have a significant impact on chemical structure. No less important, however, are the stabilizing effects of hyperconjugative delocalization and nonbonded interactions.[19,20] One example of the stabilization of a conformer through increased hyperconjugative delocalization is the "gauche effect", or the tendency of molecules to adopt the conformation that has the maximum number of gauche interactions between adjacent polar bonds.[21−28] Another example is the $n \rightarrow \pi^*$ interaction that is responsible for the Bürgi−

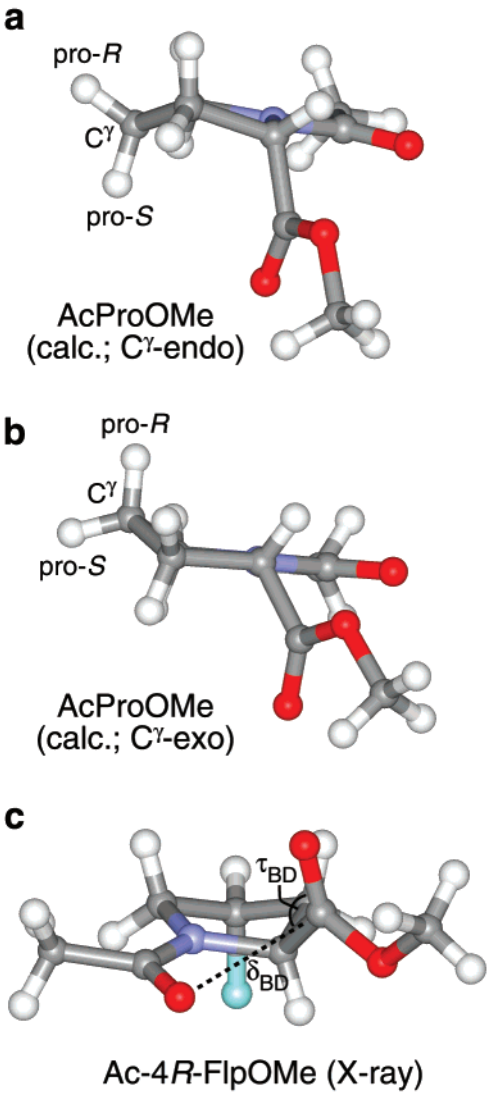

Figure 1. Structures showing the two dominant prolyl ring puckers. Calculated structures for AcProOMe in the (a) endo or "down" pucker and (b) exo or "up" pucker. Geometries were optimized fully at the B3LYP/6-31+G* level of theory. The *proR* and *proS* hydrogens are labeled. (c) Crystalline structure of Ac-4*R*-FlpOMe[32] illustrating the Bürgi−Dunitz trajectory,[29] which is the preferred angle (τ_{BD}) of the approach of a nucleophile to a distance (δ_{BD}) from a carbonyl group for an acyl transfer reaction.

(5) A 4(*R*)-Hyp residue in the Xaa position stabilizes triple helices of both $Ac(Gly\text{-}Xaa\text{-}Thr)_{10}NH_2$ and $Ac(Gly\text{-}Xaa\text{-}Thr(\beta\text{-}Gal))_{10}NH_2$ relative to a Pro residue in that position (Bann, J.; Bächinger, H. *J. Biol. Chem.* **2000**, *275*, 24466−24469).
(6) Inouye, K.; Sakakibara, S.; Prockop, D. J. *Biochim. Biophys. Acta* **1976**, *420*, 133−141.
(7) Bretscher, L. E.; Taylor, K. M.; Raines, R. T. In *Peptides for the New Millennium: Proceedings of the Sixteenth American Peptide Symposium*; Fields, G. B.; Tam, J. P.; Barany, G., Eds.; Kluwer Academic: Dordrecht, The Netherlands, 2000, pp 355−356.
(8) Raines, R. T.; Bretscher, L. E.; Holmgren, S. K.; Taylor, K. M. In *Peptides for the New Millennium: Proceedings of the Sixteenth American Peptide Symposium*; Kluwer Academic: Dordrecht, The Netherlands, 2000, pp 344−346.
(9) Bretscher, L. E.; Jenkins, C. L.; Taylor, K. M.; Raines, R. T. *J. Am. Chem. Soc.* **2001**, *123*, 777−778.
(10) Shaw, B. R.; Schurr, J. M. *Biopolymers* **1975**, *14*, 1951−1985.
(11) Fraser, R. D. B.; MacRae, T. P.; Suzuki, E. *J. Mol. Biol.* **1979**, *129*, 463−481.
(12) Okuyama, K.; Okuyama, K.; Arnott, S.; Takayanagi, M.; Kakudo, M. *J. Mol. Biol.* **1981**, *152*, 427−443.
(13) Li, M.-H.; Fan, P.; Brodsky, B.; Baum, J. *Biochemistry* **1993**, *32*, 7377−7387.
(14) Bella, J.; Eaton, M.; Brodsky, B.; Berman, H. M. *Science* **1994**, *266*, 75−81.
(15) Kramer, R. Z.; Vitagliano, L.; Bella, J.; Berisio, R.; Mazzarella, L.; Brodsky, B.; Zagari, A.; Berman, H. M. *J. Mol. Biol.* **1998**, *280*, 623−638.
(16) Nagarajan, V.; Kamitori, S.; Okuyama, K. *J. Biochem.* **1998**, *124*, 1117−1123.
(17) Okuyama, K.; Nagarajoan, V.; Kamitori, S. *Proc. Indian Acad. Sci.* **1999**, *111*, 19−34.
(18) Vitagliano, L.; Berisio, R.; Mazzarella, L.; Zagari, A. *Biopolymers* **2001**, *58*, 459−464.
(19) Pophristic, V.; Goodman, L. *Nature (London)* **2001**, *411*, 565−568.
(20) Weinhold, F. *Nature (London)* **2001**, *411*, 539−541.
(21) Wolfe, S. *Acc. Chem. Res.* **1972**, *5*, 102−111.
(22) Phillips, L.; Wray, V. J. *J. Chem. Soc., Chem. Commun.* **1973**, *173*, 90.
(23) Brunck, T. K.; Weinhold, F. *J. Am. Chem. Soc.* **1979**, *101*, 1700−1709.
(24) Olson, W. K. *J. Am. Chem. Soc.* **1982**, *104*, 278−286.
(25) Olson, W. K.; Sussman, J. L. *J. Am. Chem. Soc.* **1982**, *104*, 270−278.
(26) Murcko, M. A.; DiPaola, R. A. *J. Am. Chem. Soc.* **1992**, *114*, 10010−10018.
(27) A calculation has revealed that the fluorine-amide gauche effect is especially strong (O'Hagan, D.; Bilton, C.; Howard, J. A. K.; Knight, L.; Tozer, D. J. *J. Chem. Soc., Perkin Trans. 2* **2000**, 605−607).

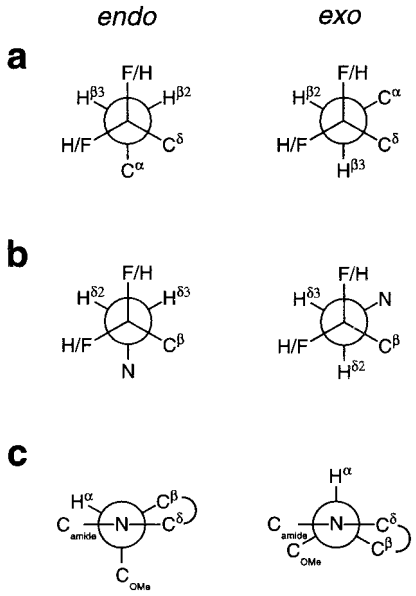

Figure 2. Newman projections about three bond axes illustrating the stereochemistry of the proline-containing model compounds (4*R*-Flp/4*S*-Flp) in their endo and exo conformations: (a) C^{γ}-C^{β}, (b) C^{γ}-C^{δ}, and (c) N−C^{α}. For simplicity, each dihedral angle is shown in its fully staggered conformation rather than its optimized geometry.

Dunitz trajectory.[29] The Bürgi−Dunitz trajectory (τ_{BD}) refers to the preferred angle at which a nucleophile approaches (to distance δ_{BD}) a carbonyl group for an acyl transfer reaction. The Bürgi−Dunitz trajectory was deduced initially from a survey of small-molecule crystal structures[30] in which potential nucleophiles are proximal to carbonyl groups, with δ_{BD} varying from 1.5 (covalently bonded) to 3.0 Å. In general, the value of τ_{BD} is not the 90° predicted from steric considerations alone.[29] Instead, the τ_{BD} value arises from maximizing the overlap between the lone pair (*n*) of the nucleophile and the antibonding π^* orbital of the carbonyl group, while minimizing steric interactions that occur when the nucleophile and carbonyl group come into close contact. The relevant n $\rightarrow \pi^*$ interaction in collagen, where the suppositious nucleophile is the amide oxygen of an Xaa_{i-1}−Pro_i peptide bond and the carbonyl group is from Pro_i, is depicted in Figure 1c.[9,31]

To determine how a γ-substitutent affects the delicate balance among these contributions (steric interactions, hyperconjugative delocalization, and nonbonded interactions), NMR spectroscopy was used to analyze the conformational energetics of a series of model compounds containing a single prolyl derivative. In addition, electronic structure calculations were carried on the model compounds as a function of their conformation. The compounds investigated were a series of *N*-acetylated prolyl methyl esters with or without a fluorine atom at either the 4*R* or the 4*S* position: *N*-acetylated prolyl methyl ester (Ac-ProOMe), *N*-acetylated 4(*R*)-fluoroprolyl methyl ester (Ac-4*R*-FlpOMe), and *N*-acetylated 4(*S*)-fluoroprolyl methyl ester (Ac-4*S*-FlpOMe). The basis for the choice of these model compounds was discussed previously.[3,32,33,] The three effects were analyzed with the natural bond orbital (NBO) paradigm.[23,34]

The NBO package is a suite of methods for describing the N-electron wave function in terms of localized orbitals or configurations that are related to chemical bonding concepts. Closely associated is the natural resonance theory (NRT),[35−37] which provides a related population weighting for localized N-electron configurational functions corresponding to the "resonance structure" picture based on the analysis of the one-electron density matrix. These resonance weights can be used to approximate a given electronic structure as the weighted average of contributions from idealized, localized Lewis resonance structures. Second-order perturbation energies that are calculated by the NBO package reflect the strength of donor−acceptor (or bond−antibond) hyperconjugative interactions between NBOs. The stabilization energies are calculated by examining all possible interactions between "filled" (donor) Lewis-type NBOs and "empty" (acceptor) non-Lewis NBOs and estimating their energetic importance by second-order perturbation theory. These interactions lead to the loss of occupancy from the localized NBOs of the idealized Lewis structure into the empty non-Lewis orbitals. Such interactions are referred to as "delocalization" corrections to the zeroth-order natural Lewis structure. In general, more delocalization interactions for a given conformation mean greater stability of that conformer. One is further able to determine with NBO analysis the effects of orbital delocalization by "deleting" certain orbitals or specific interactions between orbitals and recalculating the approximate SCF energy for the hypothetical system with the specific interaction(s) missing. Another NBO method of particular importance in this study is natural steric analysis (NSA).[38,39] In the basis of natural bond orbitals, steric interactions can be calculated by identifying interatomic "exchange repulsion" energy components associated with wave function antisymmetry. The results of the NBO analysis provide the basis for a detailed understanding of the underlying principles responsible for the conformational stability of collagen.

Experimental Section

Materials. AcProOMe, Ac-4*R*-FlpOMe, and Ac-4*S*-FlpOMe were synthesized as described previously.[9,32]

NMR Spectroscopy. NMR experiments were performed on a 3−5 mM solution of AcProOMe, Ac-4*R*-FlpOMe, or Ac-4*S*-FlpOMe in dioxane. Dioxane was chosen as the solvent because its low dielectric constant reflects the in vacuo calculations. One-dimensional (1D) NMR and two-dimensional (2D) NOESY data sets were collected on a Bruker DMX 500 spectrometer at 25 °C. 2D E.COSY-type data were collected

(28) Conformational preferences of double-helical nucleic acids have been explained in terms of the gauche effect. For leading references, see: (a) Guschlbauer, W.; Jankowski, K. *Nucleic Acids Res.* **1992**, *114*, 10010−10018. (b) Plavec, J.; Thibaudeau, C.; Chattopadhyaya, J. *J. Am. Chem. Soc.* **1994**, *116*, 6558−6560. (c) Wilds, C. J.; Damha, M. J. *Bioconjugate Chem.* **1999**, *10*, 299−305.

(29) (a) Bürgi, H. B.; Dunitz, J. D.; Shefter, E. *J. Am. Chem. Soc.* **1973**, *95*, 5065−5067. (b) Bürgi, H. B.; Dunitz, J. D.; Lehn, J. M.; Wipff, G. *Tetrahedron* **1974**, *30*, 1563−1572. (c) Bürgi, H. B.; Lehn, J. M.; Wipff, G. *J. Am. Chem. Soc.* **1974**, *96*, 1965−1966. (d) Bürgi, H. B.; Dunitz, J. D.; Shefter, E. *Acta Crystallogr. Sect. B* **1974**, *30*, 1517−1527.

(30) For a review on the correlation of crystal statics and chemical dynamics, see: Bürgi, H. B.; Dunitz, J. D. *Acc. Chem. Res.* **1963**, *16*, 153−161.

(31) This n $\rightarrow \pi^*$ interaction has been proposed to stabilize the right-handed twist found in most β-strands. Maccallum, P. H.; Poet, R.; Milner-White, E. J. *J. Mol. Biol.* **1995**, *248*, 374−384.

(32) Panasik, N., Jr.; Eberhardt, E. S.; Edison, A. S.; Powell, D. R.; Raines, R. T. *Int. J. Pept. Protein Res.* **1994**, *44*, 262−269.

(33) Eberhardt, E. S.; Panasik, N., Jr.; Raines, R. T. *J. Am. Chem. Soc.* **1996**, *118*, 12261−12266.

(34) Weinhold, F. In *Encyclopedia of Computational Chemistry*; Schleyer, P. v. R.; Allinger, N. L.; Clark, T.; Gasteiger, J.; Kollman, P. A.; Shaefer, H. F.; III, Schreiner, P. R., Eds.; John Wiley & Sons: Chichester, UK, 1998; Vol. 3, pp 1792−1811.

(35) Glendening, E. D.; Weinhold, F. *J. Comput. Chem.* **1998**, *19*, 593−609.

(36) Glendening, E. D.; Weinhold, F. *J. Comput. Chem.* **1998**, *19*, 610−627.

(37) Glendening, E. D.; Weinhold, F. *J. Comput. Chem.* **1998**, *19*, 628−646.

(38) Badenhoop, J.; Weinhold, F. *J. Chem. Phys.* **1997**, *107*, 5406−5421.

(39) Badenhoop, J. K.; Weinhold, F. *Int. J. Quantum Chem.* **1999**, *72*, 269−280.

on a DMX 400, also at 25 °C. Values of $K_{trans/cis}$, which is the cis ⇄ trans peptide bond equilibrium constant, were determined from relative peak areas in the 1D NMR spectra with peak integrals determined with the Nuts program (Acorn, Berkeley, CA). NMRPipe[40] was used to process the 2D COSY and NOESY data sets. Vicinal proton−proton couplings were obtained from analysis of E.COSY spectra.[41] Continuous probability distribution (CUPID)[42−44] analysis was then used, first for stereospecific assignment of the prochiral resonances of the prolyl rings[45] and second for determining the pucker of the five-membered rings.[46] The CUPID method uses NMR data to determine the probability distribution of rotamers. The results of the CUPID analysis were then verified by reference to the NOESY data collected with a mixing time of 2 s.

Computations. For each model compound, hybrid density functional theory (DFT) calculations, as implemented in Gaussian 98,[47] were carried out on four conformers: both ring puckers (endo and exo) and both peptide bond isomers (cis and trans). Geometry optimizations and frequency calculations were performed at the B3LYP/6-31+G* level of theory. Frequency calculations of the optimized structures yielded no imaginary frequencies, indicating a true stationary point on the potential energy surface. NBO 4.0[48] was employed to analyze the optimized structures at the more precise B3LYP/6-311+G(2d,p) level to obtain detailed information about specific orbital interactions responsible for (de)stabilizing given conformations of each molecule.

To evaluate the influence of components of a molecule on its conformation, calculations were carried out on molecular fragments (Figure 3). To make the fragments realistic, hydrogens atoms were placed at the "cleavage sites". The resulting fragments were partially optimized with respect to the new C−H or N−H bond. Fragment I, was designed to isolate interactions between the fluorine atom and the methyl ester. Conformers of Fragment I to be used for computations were created by rigidly rotating the ψ torsion angle[49] from 110 to 210° in 10° increments without further optimization. Single-point energy calculations and NBO analysis at the B3LYP/6-31+G* level were then carried out on these conformations. Fragment II, which consists of the prolyl ring without the methyl ester, was designed to isolate the effect of the methyl ester on ring pucker. The fragment II compounds were fully optimized at the B3LYP 6-31+G* level, and no imaginary frequencies were found. The methyl ester was then placed back on the ring, without further geometry optimization, to determine how the methyl ester interacts with the rest of the prolyl ring. Calculations were performed on an HP-Convex X-class Exemplar computer and an Intel-based Linux workstation.

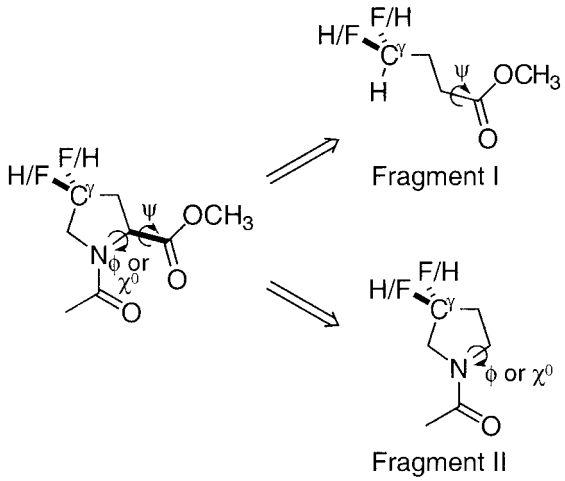

Figure 3. Structures of the parent compounds (Ac-Yaa-OMe; 4*R*-Flp/4*S*-Flp) and the two fragments used to evaluate the influence of particular components on its conformation.

Table 2. Relative Populations of the Endo and Exo Conformations of Trans Ac-Yaa-OMe Compounds Derived from NMR *J* Couplings by the CUPID Method[42−44] and $K_{trans/cis}$ Values Derived from NMR Peak Intensities[a]

	ring pucker			
Yaa	endo	exo	uncertainty	$K_{trans/cis}$
Pro	0.66	0.34	0.05	3.0
4*R*-Flp	0.14	0.86	0.08	4.0
4*S*-Flp	0.95	0.05	0.08	1.2

[a] Data were collected in dioxane at 25 °C.

Results

Conformational Population Analysis from NMR Spectroscopy. The pyrrolidine ring vicinal homonuclear coupling constants derived from 1D proton and 2D E.COSY spectra were used as the input to the version of CUPID designed for five-membered rings.[44] Signals from the prochiral hydrogens were assigned stereospecifically by an extension of the CUPID method[45] and confirmed by reference to 2D NOESY data. The results of the CUPID analysis are shown in Table 2. In solution, AcProOMe exists in both the endo and exo conformations, whereas Ac-4*R*-FlpOMe and Ac-4*S*-FlpOMe each have only one major conformation, exo for Ac-4*R*-FlpOMe and endo for Ac-4*S*-FlpOMe. The trans/cis equilibrium constants of the three compounds dissolved in dioxane were determined from integration of 1D NMR spectra (Table 2). For AcProOMe, $K_{trans/cis}$ = 3.0. A fluorine atom in the 4*R* position was found to stabilize the trans form ($K_{trans/cis}$ = 4.0 for Ac-4*R*-FlpOMe), whereas a fluorine atom in the 4*S* position stabilizes the cis form ($K_{trans/cis}$ = 1.2 for Ac-4*S*-FlpOMe).

Energy Calculations. The calculated energy difference between the two ring puckers, $\Delta(E_{endo} - E_{exo})$, for each isomer of all three compounds is listed in Table 3. In trans AcProOMe, the exo conformation is less stable than the endo by 0.41 kcal/mol. Introduction of a 4*R* fluoro substituent (Ac-4*R*-FlpOMe) makes the exo conformer 0.85 kcal/mol more stable than the endo conformer, whereas a 4*S* fluoro substitutent (Ac-4*S*-FlpOMe) makes the endo conformer 0.61 kcal/mol more stable than the exo conformer.

(40) Delagalio, F.; Grzesiek, S.; Vuister, G.; Zhu, G.; Pfeifer, J.; Baz, A. *J. Biolmol. NMR* **1995**, *6*, 277−293.
(41) Griesinger, C.; Ernst, R. R. *J. Magn. Reson.* **1987**, *75*, 474−492.
(42) Džakula, Z.; Edison, A. S.; Westler, W. M.; Markley, J. L. *J. Am. Chem. Soc.* **1992**, *114*, 6200−6207; 9727.
(43) Džakula, Z.; Westler, W. M.; Edison, A. S.; Markley, J. L. *J. Am. Chem. Soc.* **1992**, *114*, 6195−6199; 9727.
(44) Džakula, Z.; DeRider, M. L.; Markley, J. L. *J. Am. Chem. Soc.* **1996**, *1996*, 12796−12803.
(45) DeRider, M. L. Ph.D. Thesis, University of Wisconsin-Madison, 2001.
(46) Džakula, Z.; Westler, W. M.; Markley, J. L. *J. Magn. Reson.* **1996**, *111*, 109−126.
(47) *Gaussian 98* (Revision A.6), Frisch, M. J.; Trucks, G. W.; Schlegel, H. B.; Scuseria, G. E.; Robb, M. A.; Cheeseman, J. R.; Zakrzewski, V. G.; Montgomery, J. A.; Stratmann, R. E.; Burant, J. C.; Dapprich, S.; Millam, J. M.; Daniels, A. D.; Kudin, K. N.; Strain, M. C.; Farkas, O.; Tomasi, J.; Barone, V.; Cossi, M.; Cammi, R.; Mennucci, B.; Pomelli, C.; Adamo, C.; Clifford, S.; Ochterski, J.; Petersson, G. A.; Ayala, P. Y.; Cui, Q.; Morokuma, K.; Malick, D. K.; Rabuck, A. D.; Raghavachari, K.; Foresman, J. B.; Cioslowski, J.; Ortiz, J. V.; Stefanov, B. B.; Liu, G.; Liashenko, A.; Piskorz, P.; Komaromi, I.; Gomperts, R.; Martin, R. L.; Fox, D. J.; Keith, T.; Al-Laham, M. A.; Peng, C. Y.; Nanayakkara, A.; Gonzalez, C.; Challacombe, M.; Gill, P. M. W.; Johnson, B. G.; Chen, W.; Wong, M. W.; Andres, J. L.; Head-Gordon, M.; Replogle, E. S.; Pople, J. A. Gaussian, Inc., Pittsburgh, PA, 1998. For current program information, see: http://www.Gaussian.com.
(48) *NBO 4.0*, E. D. Glendening, J. K.; Badenhoop, A. E.; Reed, J. E.; Carpenter, F. Weinhold, Theoretical Chemistry Institute, University of Wisconsin-Madison, Madison, WI, 1996. For current program information, see: http://www.chem.wisc.edu/~nbo5.
(49) In AcProOMe and its derivatives, the ψ torsion angle refers to $N_i-C^{\alpha}{}_i-C'_i-O_{i+1}$.

Table 3. Calculated Energy Differences between Conformational ($\Delta(E_{endo} - E_{exo})$) and Configurational ($\Delta(E_{trans} - E_{cis})$) States of Ac-Yaa-OMe Compounds[a]

	$\Delta(E_{endo} - E_{exo})$ (kcal/mol)		$\Delta(E_{trans} - E_{cis})$ (kcal/mol)	
yaa	trans	cis	endo	exo
Pro	−0.41	−0.60	−1.20	−1.39
4*R*-Flp	0.85	1.18	−1.62	−1.29
4*S*-Flp	−0.61	−1.99	−0.13	−1.51

[a] Data are ZPE-corrected energies from DFT calculations with B3LYP at 6-311+G(2d,p).

The calculated energy difference between the two configurational isomers, $\Delta(E_{cis} - E_{trans})$, for each of the three compounds in both ring puckers is also listed in Table 3. For all conformations, the trans isomer is more stable than the cis isomer. The trans/cis energy differences for both ring pucker conformations of AcProOMe and Ac-4*R*-FlpOMe range from 1.20 to 1.62 kcal/mol. In Ac-4*S*-FlpOMe, the trans/cis energy difference for Ac-4*S*-FlpOMe is about 1.51 kcal/mol in its exo conformation, but only 0.13 kcal/mol in its endo conformation.

The second-order perturbative estimates of the stabilization energy between the $C^{\gamma}-F$ antibonding orbital and the bonds that are anti to the $C^{\gamma}-F$ bond are listed in Table 4. The corresponding delocalization energies were calculated with NBO. In Ac-4*R*-FlpOMe exo, the second-order perturbative estimates of hyperconjugative delocalization between the $C^{\gamma}-F$ antibond and the two carbon−hydrogen bonds are 4.53 and 4.08 kcal/mol (Table 4). In contrast, the second-order perturbative estimates of hyperconjugative delocalization between the $C^{\gamma}-F$ antibond and the two bonds anti to the $C^{\gamma}-F$ bond in Ac-4*R*-FlpOMe endo are 2.89 and 1.52 kcal/mol. In Ac-4*S*-FlpOMe endo, the second-order perturbative estimates of hyperconjugative delocalization between the $C^{\gamma}-F$ antibond and the two carbon−hydrogen bonds are 4.22 and 2.46 kcal/mol. In contrast, the second-order perturbative estimates of hyperconjugative delocalization between the $C^{\gamma}-F$ antibond and the two bonds *anti* to the $C^{\gamma}-F$ bond in Ac-4*S*-FlpOMe exo are 2.91 and 1.40 kcal/mol.

NBO can also be used to determine the effects of orbital delocalization by "deleting" certain orbitals or specific interactions between orbitals and recalculating the approximate SCF energy for the hypothetical system. The calculated deletion energies provide a measure of the loss of stabilization resulting from deletion of the $C^{\gamma}-F$ antibonding orbital. Deletion of the $C^{\gamma}-F$ antibonding orbital has more of a destabilizing effect on Ac-4*R*-FlpOMe exo (17.9 kcal/mol) and Ac-4*S*-FlpOMe endo (17.1 kcal/mol) than on Ac-4*R*-FlpOMe endo (14.1 kcal/mol) or Ac-4*S*-FlpOMe exo (14.0 kcal/mol),[45] which is qualitatively consistent with the second-order estimates (Table 4).

Geometry Calculations. Bond orders were calculated with the NRT routine in NBO. Natural charges were also calculated with NBO. The calculated effects on the geometry (i.e., bond length, bond order, and natural charge) of the trans Ac-Yaa-OMe compounds that can be attributed to increased hyperconjugative delocalization into the $C^{\gamma}-F$ antibonding orbital as the result of introducing γ-substituents are listed in Table 5. Other manifestations of hyperconjugative delocalization from the bridging oxygen of the ester to the π^* orbital of the ester carbonyl group are also listed in Table 5.

The Ramachandran plot in Figure 4 summarizes the ring pucker and ϕ and ψ torsion angles from the present computational results and from X-ray crystallographic data on collagen-like peptides. The interrelationship between the ϕ and ψ angles is demonstrated further in the insets in Figure 4, which depicts the energetic consequences of varying these angles but holding the rest of the geometry constant in AcProOMe trans endo (Figure 4a) and trans exo (Figure 4b).

The calculated energies of fragment I compounds as a function of ψ are depicted in Figure 5a. Only the fragments derived from Ac-4*S*-FlpOMe endo exhibit a large energy change as ψ decreases from 180 to 100°. The dependence on ψ of the NSA-derived steric exchange energy between the fluorine atom and the ester oxygens of the model compounds is shown in Figure 5b. Calculated geometry values (ϕ, ψ, τ_{BD}, and δ_{BD}) and the stabilization energies for the trans isomers of AcProOMe exo, AcProOMe endo, Ac-4*R*-FlpOMe exo, and Ac-4*S*-FlpOMe endo are summarized in Table 6.

Discussion

Hyperconjugative delocalization has a marked effect on the relative stabilities of molecular conformations,[19,20] including those of γ-substituted prolyl rings. The preferred conformation of these rings depends on the electronegativity and stereochemistry of the γ-substituent (Table 2).[50] The ring pucker preference of γ-substituted prolyl rings can be explained by invoking the "gauche effect"[3,33]—the tendency of molecules to adopt the conformation that has the maximum number of gauche interactions between adjacent polar bonds. In a γ-fluorinated pyrrolidine ring, the preferred pucker will be the one that aligns the $C^{\gamma}-F$ bond anti to C−H bonds. As is apparent from the Newman projections in Figure 2, in Ac-4*R*-FlpOMe exo and Ac-4*S*-FlpOMe endo, the $C^{\gamma}-F$ bonds are anti to the $C^{\beta}-H^{\beta 2}$ and $C^{\delta}-H^{\delta 2}$ bonds, but in Ac-4*R*-FlpOMe endo and Ac-4*S*-FlpOMe exo, the $C^{\gamma}-F$ bonds are anti to bonds to other electronegative atoms, $C^{\beta}-C^{\sigma}$ and $C^{\delta}-N$. The $C^{\gamma}-F$ antibonding orbital is better able to accept electron density from the carbon−hydrogen bonds in Ac-4*R*-FlpOMe exo and Ac-4*S*-FlpOMe endo than from the carbon−carbon and carbon−nitrogen bonds in Ac-4*R*-FlpOMe endo and Ac-4*S*-FlpOMe exo, as is apparent from the second-order estimates and deletion energies calculated by NBO (Table 4).

One effect of hyperconjugative delocalization is a dramatic deviation in geometry from idealized Lewis structures. As the amount of delocalization into the $C^{\gamma}-F$ antibonding orbital increases, the bond length of the $C^{\gamma}-F$ bond increases and the bond order decreases. In their trans conformation, the calculated $C^{\gamma}-F$ bond lengths in Ac-4*R*-FlpOMe exo (1.4121 Å) and Ac-4*S*-FlpOMe endo (1.4105 Å) are longer than those in Ac-4*R*-FlpOMe endo (1.4036 Å) or Ac-4*S*-FlpOMe exo (1.4003 Å) (Table 5).

The $C^{\gamma}-F$ bond orders determined from NBO (Table 5) also show the effects of increased hyperconjugative delocalization. The $C^{\gamma}-F$ bond orders in Ac-4*R*-FlpOMe exo (1.0021) and Ac-4*S*-FlpOMe endo (1.0038) are smaller than those in Ac-4*R*-FlpOMe endo (1.0090) or Ac-4*S*-FlpOMe exo (1.0089). Moreover, the $C^{\gamma}-F$ bond is expected to be more anionic in character with increased hyperconjugative delocalization. The natural charge of fluorine from NBO is more negative in Ac-4*R*-FlpOMe exo (−0.4097) and Ac-4*S*-FlpOMe endo (−0.4058)

(50) Gerig, J. T.; McLeod, R. S. *J. Am. Chem. Soc.* **1973**, *95*, 5725−5729.

Table 4. Second-Order Perturbative Estimates of Donor−Acceptor Interactions in the NBO Basis for the Trans Configurations of Ac-Yaa-OMe Compounds in Their Endo and Exo Conformations

	endo			exo		
Yaa	donor	acceptor	stabilization energy (kcal/mol)	donor	acceptor	stabilization energy (kcal/mol)
4*R*-Flp	$\sigma(C^{\beta}-C^{\alpha})$	$\sigma^*(C^{\gamma}-F)$	2.89	$\sigma(C^{\beta}-H^{\beta 3})$	$\sigma^*(C^{\gamma}-F)$	4.53
	$\sigma(C^{\delta}-N)$	$\sigma^*(C^{\gamma}-F)$	1.52	$\sigma(C^{\delta}-H^{\delta 2})$	$\sigma^*(C^{\gamma}-F)$	4.08
4*S*-Flp	$\sigma(C^{\beta}-H^{\beta 2})$	$\sigma^*(C^{\gamma}-F)$	4.22	$\sigma(C^{\beta}-C^{\alpha})$	$\sigma^*(C^{\gamma}-F)$	2.91
	$\sigma(C^{\delta}-H^{\delta 3})$	$\sigma^*(C^{\gamma}-F)$	2.46	$\sigma(C^{\delta}-N)$	$\sigma^*(C^{\gamma}-F)$	1.40

Table 5. Bond Lengths, Bond Orders, and Natural Charges for the Trans Conformation of Ac-Yaa-OMe Compounds as Determined from Analysis of DFT Data

	Yaa and its ring conformation					
	Pro		4*R*-Flp		4*S*-Flp	
bond or atom	endo	exo	endo	exo	endo	exo
bond length (Å)						
$C^{R}{=}O$	1.2135	1.2131	1.2141	1.2135	1.2094	1.2124
$C^{R}-O_{ester}$	1.3468	1.3454	1.3431	1.3427	1.3495	1.3438
$C^{\gamma}-F$			1.4036	1.4036	1.4105	1.4008
bond order						
$C^{R}{=}O$	1.9546	1.9537	1.9497	1.9524	1.9629	1.9519
$C^{R}-O_{ester}$	1.0650	1.0636	1.0694	1.0682	1.0588	1.0662
$C^{\gamma}-F$			1.0090	1.0021	1.0038	1.0089
natural charge						
C^{R}	0.8333	0.8393	0.8320	0.8379	0.8295	0.8372
$O^{R}_{carbonyl}$	−0.6174	−0.6188	−0.6193	−0.6196	−0.5947	−0.6139
O^{R}_{ester}	−0.5574	−0.5541	−0.5526	−0.5500	−0.5660	−0.5530
F	−	−	−0.4009	−0.4097	−0.4058	−0.3976

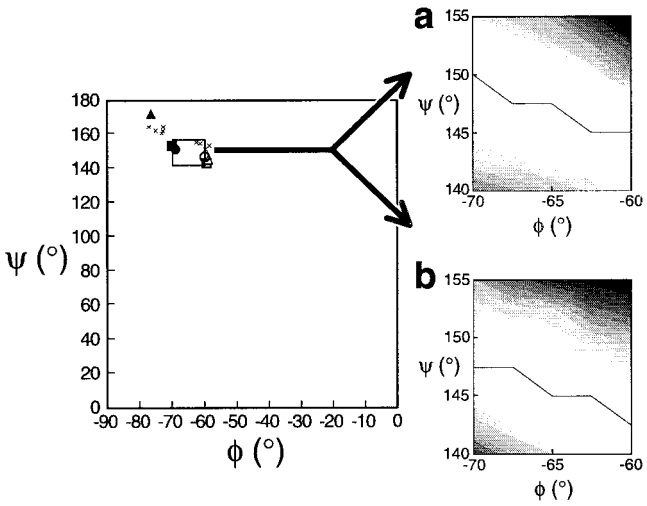

Figure 4. Ramachandran plot showing the ϕ and ψ angles of the minimal energy structures calculated herein (filled for endo; open for exo): AcProOMe (■;□), Ac-4*R*-FlpOMe (▲;△), and Ac-4*S*-FlpOMe (●;○). Shown for comparison are the ϕ and ψ angles found in X-ray crystallographic studies of collagen-like peptides (×).[11,12,14−18] Insets: Calculated energy contours for relevant ϕ and ψ angles of (a) AcProOMe trans endo and (b) AcProOMe trans exo.

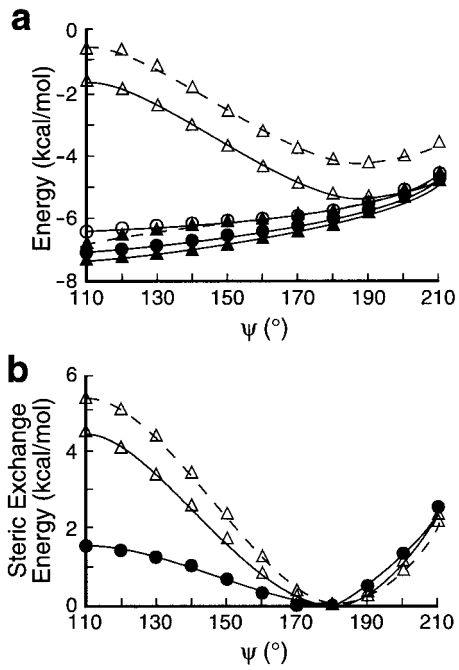

Figure 5. Plot showing the effect of the ψ angle on the energies of Ac-4*R*-FlpOMe trans exo (●), Ac-4*R*-FlpOMe trans endo (▲), Ac-4*S*-FlpOMe trans exo (○), and Ac-4*S*-FlpOMe trans endo (△): (a) relative energies and (b) steric exchange energies. Dashed lines indicate the energies of structures obtained upon inverting the stereochemistry of fluorine from 4*R* to 4*S* (or vice versa), but holding the rest of the geometry constant. In panel b, only the major conformers are shown.

than in Ac-4*R*-FlpOMe endo (−0.4009) or Ac-4*S*-FlpOMe exo (−0.3976) (Table 5).

Effect of Steric Interactions on Ring Conformations and ϕ Angles. A correlation has been discovered between ring pucker and the ϕ torsion angle ($C'_{i-1}-N_i-C^{\alpha}_i-C'_i$) of proline-containing peptides in the Cambridge Structural Database and proteins in the Protein Data Bank.[18] Specifically, exo ring conformations are accompanied by less negative ϕ angles than are endo ring conformations. The basis for this correlation had been unknown.

NBO provides an explanation for the correlation of ring pucker and ϕ angle (Figure 4). The synchronous χ^0 torsional angle ($C_i^{\beta}-C_i^{\alpha}-N_i-C_i^{\delta}$) of proline, which is likewise constrained by the pyrrolidine ring, is −13.9° in AcProOMe trans endo and 0.6° in AcProOMe trans exo. A computational study

Table 6. Geometric Parameters for the Trans Configurations of Ac-Yaa-OMe Compounds Calculated from Fully Optimized Geometries by DFT with B3LYP at 6-31+G* and Stabilization Energies Calculated by NBO with B3LYP at 6-311+G(2d,p) for the Lone Pair of the Amide Oxygen Donating to the π^* Orbital of the Ester Carbonyl Group[a]

Yaa	conformer	ϕ (deg)	ψ (deg)	τ_{BD} (deg)	δ_{BD} (Å)	stabilization energy (kcal/mol)
Pro	exo	−58.61	143.02	99.35	2.87	1.29
4*R*-Flp	exo	−59.22	140.79	100.74	2.86	1.38
Pro	endo	−69.95	152.07	99.43	3.06	0.42
4*S*-Flp	endo	−76.44	171.95	88.76	3.23	0.07

[a] Data are only for the major conformers.

was carried out on both endo and exo conformations of a fragment of AcProOMe that lacks the methyl ester (fragment II, Figure 3). The geometry of both conformations was optimized fully. Unlike in AcProOMe, the ring conformers of fragment II are enantiomers, and were found to be of equivalent energy to within 1×10^{-5} kcal/mol.[45] Furthermore, both χ^0 torsional angles are approximately equal in absolute magnitude to that in AcProOMe trans endo (Figure 1a), $\chi^0 = -10.6°$ in fragment II endo and $\chi^0 = 12.9°$ in fragment II exo. In AcProOMe trans exo (Figure 1b), the bulky methyl ester comes in close contact with the amide oxygen. The torsion angle from the amide carbon to the hydrogen that replaces the methyl ester in fragment II ($C'_{i-1}-N_i-C^{\alpha}_i-H_i^R$) is referred to here as pseudo ϕ. The value of pseudo ϕ for fragment II exo is $-47°$, whereas the corresponding value of the ϕ angle for AcProOMe exo is $-58°$. This deviation in ϕ serves to increase the distance between the two carbonyl groups of AcProOMe. In the trans exo conformation of reconstituted AcProOMe ($\chi^0 = 12.9°$ and $\phi = -47°$), the ester carbon is only 2.7 Å away from the amide oxygen, and as expected, NSA shows a large steric repulsion (1.75 kcal/mol) between the p-type lone pair of the amide oxygen and the π bond of the ester carbonyl group. If the ϕ angle alone is decreased to $-57°$, steric repulsion between the lone pair and the π bond decreases to 0.60 kcal/mol. To relieve some of the steric strain, the ϕ angle of the exo conformer becomes more negative, and as a direct consequence, the χ^0 dihedral angle decreases, causing a flattening of the ring that is apparent in Figure 1b. In effect, the flattening of the ring acts to dissipate some of the steric strain between the two carbonyl groups. The increased strain on the ring causes the exo conformation to be slightly less favored energetically than the endo conformation. The difference in the total exchange energy from NSA in NBO between the fully optimized AcProOMe trans exo and trans endo is 1.24 kcal/mol, with AcProOMe trans exo being the more sterically strained conformer. The difference in the total exchange energy can be attributed largely to steric strain between the two carbonyl groups and the $C^{\delta}-C^{\gamma}$ and $C^{\delta}-N$ bonds.

Effect of $n \rightarrow \pi^*$ Interaction (Bürgi−Dunitz Trajectory) on ψ Angles. The ϕ and ψ torsion angle from the present computational results and from previous X-ray crystallographic data on collagen-like peptides are summarized in the Ramachandran plot in Figure 4.[49] In the exo ring pucker, the smaller ψ angles are accompanied by less negative ϕ angles. The energetic consequences of varying the peptide torsion angles for AcProOMe trans endo (Figure 4a) and trans exo (Figure 4b), but holding the rest of the geometry constant, demonstrate further the relationship between the ϕ and ψ angles. In the trans isomer, this relationship can be rationalized in terms of the n $\rightarrow \pi^*$ interaction that is responsible for the Bürgi−Dunitz trajectory (Figure 1c).[51] Decreasing the ϕ angle without decreasing the ψ angle changes the angle at which the amide oxygen approaches the ester carbonyl group. In both the endo and exo conformations of trans AcProOMe and trans Ac-4*R*-FlpOMe, the τ_{BD} angles from the amide oxygen to the ester carbonyl group are similar (∼100°; Table 6) and only slightly smaller than the optimal Bürgi−Dunitz trajectory ($\tau_{BD} = 109°$) for the attack of a nucleophile on a carbonyl group.[29]

The distance δ_{BD} between the nucleophile and the electrophilic carbonyl carbon makes an important contribution to the stabilization that arises from the n $\rightarrow \pi^*$ interaction. In the exo conformation of AcProOMe, the distance between the amide oxygen and the ester carbon is much shorter than in the endo conformation (Table 6). Thus, more stabilization of the trans isomer is expected in the exo conformation from the delocalization of the lone pair of the amide oxygen into the π^* orbital of the ester carbonyl group. Second-order perturbation estimates from NBO do indeed show greater stabilization from delocalization in AcProOMe trans exo (1.29 kcal/mol) than in AcProOMe trans endo (0.42 kcal/mol) (Table 6).[52]

Distortion of the ψ Angle in Ac-4*S*-FlpOMe by Steric Effects. The Ramachandran plot in Figure 4 shows that the ψ angle is significantly larger in Ac-4*S*-FlpOMe trans endo than in AcProOMe trans endo or Ac-4*R*-FlpOMe trans endo. The larger ψ value for Ac-4*S*-FlpOMe trans endo arises from the steric interaction of the fluorine atom and the methyl ester on the pyrrolidine ring that is reminiscent of an unfavorable 1,3-diaxial interaction in a cyclohexane ring. The fluorine atom, which is in the 4*S* position in the endo conformation, causes the methyl ester to move away (i.e., to larger ψ values). If Ac-4*S*-FlpOMe trans endo were to adopt the low-energy geometry of AcProOMe trans endo or Ac-4*R*-FlpOMe trans endo (i.e., with $\psi = 150°$), then the distance between the fluorine and carbonyl oxygen would be only 3.03 Å. Instead, at its minimum energy, Ac-4*S*-FlpOMe trans endo has $\psi = 170°$ and the fluorine−oxygen distance is 3.33 Å.

This steric effect is less prominent in AcProOMe and Ac-4*R*-FlpOMe. Although the van der Waals radii of fluorine and hydrogen are similar (1.35 and 1.30 Å, respectively), the carbon−fluorine bond length (1.4 Å) is greater than the carbon−hydrogen bond length (1.1 Å). As a consequence of the shorter bond length, the analogous hydrogen in the endo conformations of AcProOMe and Ac-4*R*-FlpOMe is simply farther from the ester carbonyl oxygen at smaller ψ values than is the fluorine in Ac-4*S*-FlpOMe.

The steric interaction between the fluorine and the methyl ester in Ac-4*S*-FlpOMe trans endo at low values of ψ has been examined by NSA analysis of fragment I model compounds (Figure 3). Figure 5a shows the energies of fragment I compounds as a function of ψ. Only the fragments derived from Ac-4*S*-FlpOMe endo encounter a large energy barrier as ψ decreases from 180° to 100°. Figure 5b shows the effect of ψ on the NSA-derived steric exchange energy for the ester oxygens

(51) The Bürgi−Dunitz trajectory pertains only to the trans isomer of an $Xaa_{i-1}-Pro_i$ peptide bond, because in the cis isomer, C^{α} rather than the amide oxygen of Xaa_{i-1} is proximal to the carbonyl group.

(52) This decrease in n $\rightarrow \pi^*$ overlap provides an explanation for the observation that endo ring puckers tend to coincide with cis rather than trans prolyl peptide bonds in crystalline proteins (Milner-White, J. E.; Bell, L. H.; Maccallum, P. H. *J. Mol. Biol.* **1992**, *228*, 725−734).

and fluorine atom.[53] Steric interactions between the fluorine and the ester oxygens account qualitatively for the total energy differences.

Additional model compounds were used to examine the possibility that effects, other than steric hindrance between the fluorine atom and the ester oxygens, contribute to the energy barrier in Figure 5. The H^{γ} and F atoms of fragment I from Ac-4*R*-FlpOMe and Ac-4*S*-FlpOMe endo were exchanged, and the C−F and C−H bonds lengths were allowed to optimize, while the rest of the geometry was held constant. This modification essentially switched Ac-4*R*-FlpOMe endo into Ac-4*S*-FlpOMe endo, and vice versa. These fragments, denoted respectively as "4*R*-from-4*S*" and "4*S*-from-4*R*", are represented by the dashed lines in Figure 5. Because the energies of 4*R*-from-4*S* resemble those of Ac-4*R*-FlpOMe fragments and the energies of 4*S*-from-4*R* resemble those of Ac-4*S*-FlpOMe fragments, it is possible to conclude that the steric interactions of Ac-4*S*-FlpOMe endo, which become maximal at $\psi = 110°$, are due solely to the stereochemistry of the fluorine atom and not other geometrical considerations.

As discussed above, the optimal ψ value for Ac-4*S*-FlpOMe endo is larger than that for Ac-4*R*-FlpOMe or AcProOMe, owing to steric interactions between the fluorine and ester oxygens. Because the pyrrolidine ring limits any large compensatory change in the ϕ angle, the τ_{BD} angle is 88°, which is a suboptimal Bürgi−Dunitz trajectory. In addition, as δ_{BD} increases, the overlap between the lone pair of the amide oxygen and the π^* orbital of the ester carbonyl group decreases. The second-order perturbative estimate of this interaction is 0.07 kcal/mol for Ac-4*S*-FlpOMe trans endo, as compared to 0.42 kcal/mol for AcProOMe trans endo (Table 6).[52,54,55]

Effect of ψ Angle on Ester Resonance Stabilization. As ψ increases toward 180°, the ester carbonyl oxygen of Ac-4*S*-FlpOMe trans endo approaches the amide oxygen. As a consequence, the π^* orbital of the ester carbonyl group is less able to accept electron density from the lone pair of the bridging oxygen of the ester (Figure 6), and resonance stabilization decreases. In the cis isomer, as ψ approaches 180°, the ester carbonyl group approaches C^{α} of the preceding residue, which has little effect on resonance stabilization. Thus, the ester carbonyl group in Ac-4*S*-FlpOMe trans endo should have greater double-bond character than the ester carbonyl group in the cis endo conformation. Bond orders and bond lengths computed in NBO confirm this expectation (Table 5).

As a consequence of differences in electron delocalization, the ester carbonyl oxygen should be less negative in Ac-4*S*-FlpOMe trans endo than in Ac-4*R*-FlpOMe trans endo. NBO confirms a charge difference of 0.0246 (Table 5). Correspondingly, the bridging oxygen of the ester is more negative in Ac-4*S*-FlpOMe trans endo than in Ac-4*R*-FlpOMe trans endo. Because carbonyl stretching vibrations decrease with decreasing carbonyl bond order, these vibrations should be at lower frequency for the ester in Ac-4*R*-FlpOMe than in Ac-4*S*-FlpOMe. This expectation is in gratifying agreement with experimental IR data.[9]

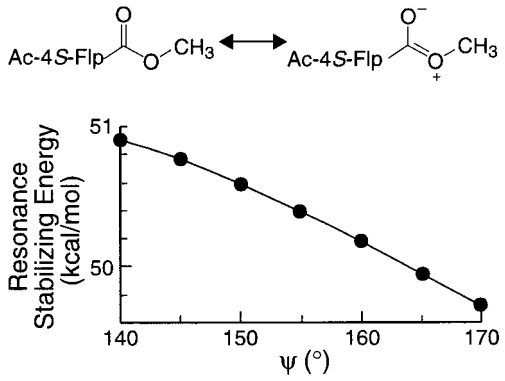

Figure 6. Plot showing the effect of the ψ angle on the second-order perturbation energies of hyperconjugative delocalization from the bridging oxygen of the ester to the π^* orbital of the ester carbonyl group in Ac-4*S*-FlpOMe.

Conclusions

To understand how a γ-substituent affects collagen stability (Table 1), one first must determine how a γ-substituent influences the conformational equilibria (ring pucker and peptide bond trans/cis ratio) of the relevant proline residues. Both the experimental and computational results herein show that a prolyl ring without a fluorine substituent has a slight preference for the endo ring pucker (Tables 2 and 3). Likewise, the preference of Ac-4*R*-FlpOMe for exo and Ac-4*S*-FlpOMe for endo is evident both in the relative populations from NMR experiments and in the relative energies derived from electronic structure calculations. The ring pucker preference of a γ-fluorinated prolyl ring can be explained in terms of the gauche effect, which, in turn, is a simple consequence of hyperconjugative interactions.

To obtain a more complete picture of collagen stability, one must include the ϕ and ψ torsion angles, which correlate with the ring pucker (Figure 4). The exo ring pucker has a smaller ψ and a less negative ϕ than does the endo ring pucker. Minimization of steric strain between the two carbonyl groups and the $C^{\delta}-C^{\gamma}$ and $C^{\delta}-N$ bonds provides a rationale for these correlations.

In addition to affecting ring pucker, the stereochemistry of a γ-substitutent affects $K_{trans/cis}$. Relative to AcProOMe ($K_{trans/cis} = 3.0$ in dioxane), Ac-4*R*-FlpOMe increases $K_{trans/cis}$ (4.0), and Ac-4*S*-FlpOMe decreases $K_{trans/cis}$ (1.2) (Table 2).[8,9,54] The stabilization of the trans isomer of Ac-4*R*-FlpOMe relative to AcProOMe arises from the effect of ring pucker on the interaction between the two carbonyl groups, as expected from a more optimal $n \rightarrow \pi^*$ interaction (Bürgi−Dunitz trajectory). Because the exo ring pucker allows for increased hyperconjugative delocalization of the lone pair of the amide oxygen into the π^* orbital of the ester carbonyl group, Ac-4*R*-FlpOMe, which exists almost exclusively in the exo pucker, has a larger trans/cis ratio than does AcProOMe, which exists in both exo and endo ring puckers (Table 2). In Ac-4*S*-FlpOMe endo, both a less optimal $n \rightarrow \pi^*$ interaction and additional destabilizing interactions are responsible for the decrease in the trans/cis ratio.

Thus, the pucker of the pyrrolidine ring in a γ-substituted proline residue, its ϕ and ψ torsion angles, and its peptide bond trans/cis ratio are interdependent parameters. The interplay between these parameters is responsible for the contribution of

(53) The ϕ torsion angle is not relevant for fragment I compounds because the amide is absent.

(54) The biosynthetic replacement of a cis Pro residue with a 4*S*-Flp residue enhances the conformational stability of a variant of the protein barstar (Renner, C.; Alefelder, S.; Bae, J. H.; Budisa, N.; Huber, R.; Moroder, L. *Angew. Chem., Int. Ed. Engl.* **2001**, *40*, 923−925).

(55) 4(*R*)-Aminoproline in the Yaa position stabilizes collagen triple helices more at low pH than at high pH (Babu, I. R.; Ganesh, K. N. *J. Am. Chem. Soc.* **2001**, *123*, 2079−2080). The effect of pH on the value of $K_{trans/cis}$ or the ring pucker of 4(*R*)-aminoproline residues is unknown.

a γ-substituted proline residue to the conformational stability of the collagen triple helix. This interplay, which results largely from hyperconjugative delocalization, has been examined herein by detailed electronic structure calculations. The results of these calculations provide a picture of collagen stability that is in agreement with experimental data.

Acknowledgment. We are grateful to Z. Džakula, S. K. Holmgren, and S. M. Tobias for help in the initial stages of the work described herein. This work was supported by Grant AR44276 (NIH) and a Biomedical Science Grant (Arthritis Foundation) to R.T.R. S.J.W. was supported by a Molecular Biophysics Training Grant GM08293 (NIH). M.J.W. was supported by a Hilldale Undergraduate/Faculty Research Fellowship from the University of Wisconsin—Madison. Equipment in the National Magnetic Resonance Facility at Madison (NMRFAM) was purchased with funds from the University of Wisconsin—Madison, the NSF Biological Instrumentation Program (DMB-8415048), NIH Biomedical Research Technology Program (RR 02301), NIH Shared Instrumentation Program (RR 02781), and the U.S. Department of Agriculture.

Supporting Information Available: Tables giving SCF energies and vicinal homonuclear couplings of Ac-Yaa-OMe with Yaa = Pro, 4*R*-Flp, and 4*S*-Flp, along with figures showing 1D NMR and representative E.COSY-type spectra. This material is available free of charge via the Internet at http://pubs.acs.org.

JA0166904